
Laplacian Features for Learning with Hyperbolic Space

Tao Yu

Department of Computer Science
Cornell University
tyu@cs.cornell.edu

Christopher De Sa

Department of Computer Science
Cornell University
cdesa@cs.cornell.edu

Abstract

Due to its geometric properties, hyperbolic space can support high-fidelity embeddings of tree- and graph-structured data. As a result, various hyperbolic networks have been developed which outperform Euclidean networks on many tasks: e.g. hyperbolic graph convolutional networks (GCN) can outperform vanilla GCN on some graph learning tasks. However, most existing hyperbolic networks are complicated, computationally expensive, and numerically unstable—and they cannot scale to large graphs due to these shortcomings. With more and more hyperbolic networks proposed, it is becoming less and less clear what key component is necessary to make the model behave. In this paper, we propose HyLa, a simple and minimal approach to using hyperbolic space in networks: HyLa maps once from a hyperbolic-space embedding to Euclidean space via the eigenfunctions of the Laplacian operator in the hyperbolic space. We evaluate HyLa on graph learning tasks including node classification and text classification, where HyLa can be used together with any graph neural networks. When used with a linear model, HyLa shows significant improvements over hyperbolic networks and other baselines.

1 Introduction

Graph learning is a growing area in modern machine learning. Data in many ML tasks take the form of graph structures, such as citation networks [29], social networks [15], and biological networks [26]. A range of problems—including node classification, link prediction, relation extraction and text classification—involves handling, predicting and classification with graph data as inputs.

An important class of model proposed in graph learning is the graph convolutional neural network (GCN) [18, 9], which is a variant of convolutional networks. This class of model achieves state-of-the-art results for tasks including semi-supervised learning for node classification tasks, supervised learning for graph-level classification, and unsupervised learning for graph embedding. Building on the original GCN, there have been many more complex graph networks and variants developed, such as the graph attention networks (GAT) [35], FastGCN [7], GraphSage [13], and others [36, 39]. These models work by embedding nodes or features in Euclidean space. However, embedding graphs in this way can have significant drawbacks, as embedding graphs in Euclidean space can cause large distortion, especially for tree-like graphs [8, 25].

An alternative approach is embedding into hyperbolic space [5], a homogeneous Riemannian manifold of constant negative curvature. Hyperbolic space is well-suited for embedding some (e.g. tree-) graph-structured data due to its geometric properties [4, 27]. A classic result of Sarkar [28] shows that it is possible to embed trees into even two-dimensional hyperbolic space with arbitrarily low distortion, which is not possible for Euclidean space of any dimension. Empirically, hyperbolic embeddings also enable extraordinary performance gains on some graph tasks, such as graph embedding, link prediction, and hierarchical inference [22, 23].

Another usage of hyperbolic space in machine learning is the development of hyperbolic neural networks (HNN), first proposed by Ganea et al. [10]. An active line of research has developed various versions of hyperbolic networks, including HNN++ by Shimizu et al. [30], hyperbolic variational auto-encoders (HVAE [21]), hyperbolic attention networks (HATN [12]), hyperbolic graph convolutional networks (HGCN [6]), hyperbolic graph neural networks (HGNN [19]), and hyperbolic graph attention networks (HGAT [44]). The strong empirical results of HGCN and HGNN in particular on node classification, link prediction, and molecular-and-chemical-property prediction show the power of hyperbolic geometry for graph learning.

However, since hyperbolic space is not a vector space, operations such as addition and multiplication are not well-defined. Neither are matrix-vector multiplication and convolution, which are key components of Euclidean Neural networks and essential for generalizing them to hyperbolic networks. Several approaches are proposed, the most popular of which is to treat hyperbolic space as a gyrovector space by equipping it with non-commutative, non-associative versions of addition and multiplication, allowing hyperbolic points to be processed as activations in a neural network. As we will discuss in Section 2, these approaches complicate the usage of hyperbolic geometry in neural networks because they require the imposition of extra “structure” on hyperbolic space beyond its properties as a manifold. With more and more hyperbolic networks proposed, it’s becoming less and less clear where the real benefits of the new mechanisms are coming from. A second problem with approaches that use points in hyperbolic space as activations, is that these points can stray far from the origin (just as Euclidean neural networks require high dynamic range [16]), especially for deeper networks. This can cause significant numerical issues when the space is represented with ordinary floating point numbers: the representation error is unbounded and can grow exponentially with distance from the origin. Much hyperparameter tuning is required to avoid this “NaN problem” [27, 41, 42]. These issues motivate the development of a simpler methodology for using hyperbolic space in networks.

In this paper, we propose a simple and natural approach, HyLa, to adopting hyperbolic geometry in networks with applications in graph learning. The main idea is to use hyperbolic space only in an initial learned embedding layer which is immediately mapped to features in Euclidean space (which are then processed normally by a downstream model). This avoids the issues above as (1) we only augment hyperbolic space \mathbb{H} with a feature map $\mathbb{H} \rightarrow \mathbb{R}^d$ rather than some more complicated structure, and (2) the points in hyperbolic space cannot “blow up” with depth, as they are only used at the first layer. The “trick” to getting this simple approach to work well in practice is the choice of feature map from \mathbb{H} to \mathbb{R}^d : our method, HyLa, uses the eigenfunctions of the Laplace-Beltrami operator in the hyperbolic space, which are the natural basis functions for Fourier analysis on \mathbb{H} . This approach is inspired by the random Fourier feature method [24], which uses eigenfunctions of the Laplace operator in Euclidean space to derive features. We make following contributions:

- We propose HyLa, a simple methodology for machine learning with hyperbolic space by mapping *once* from learned hyperbolic embeddings to Euclidean space, using the eigenfunctions of the Laplacian in hyperbolic space as features.
- We show how to use HyLa for end-to-end graph learning in transductive and inductive settings. As it only affects the initial embedding layer, HyLa can be used with any graph learning models.
- We demonstrate empirically that HyLa scales well to large graphs. When used together with a simple linear downstream model, HyLa outperforms existing hyperbolic graph neural networks. HyLa serves as an important hyperbolic baseline to compare with due to its simple implementation.
- We show that HyLa enjoys a faster computation and less memory budget than hyperbolic networks.

2 Background and Related Work on Learning in Hyperbolic Space

Hyperbolic space. n -dimensional hyperbolic space \mathbb{H}_n is usually defined and used via a model, a representation of \mathbb{H}_n within a Euclidean space. Common models include the Poincaré ball [10, 22] and Lorentz hyperboloid model [23, 6]. We develop our approach using the Poincaré ball model, but our methodology is independent of the underlying model and can be applied to other models.

The Poincaré ball model of \mathbb{H}_n is the Riemannian manifold (\mathcal{B}^n, g_p) with $\mathcal{B}^n = \{\mathbf{x} \in \mathbb{R}^n : \|\mathbf{x}\| < 1\}$ being the open unit ball and the Riemannian metric being $g_p(\mathbf{x}) = 4(1 - \|\mathbf{x}\|^2)^{-2}g_e$, where g_e is the Euclidean metric. The corresponding metric distance on \mathcal{B}^n is

$$d_p(\mathbf{x}, \mathbf{y}) = \operatorname{arcosh} \left(1 + 2 \frac{\|\mathbf{x} - \mathbf{y}\|^2}{(1 - \|\mathbf{x}\|^2)(1 - \|\mathbf{y}\|^2)} \right).$$

The use of hyperbolic space for embedding tasks is straightforward when the loss is a function of hyperbolic distances [22, 23]: here hyperbolic space is treated only as a manifold object and learning can proceed via standard Riemannian gradient descent. Using this methodology, hyperbolic embeddings of hierarchical data (e.g. tree and graphs) achieve great improvements with respect to both embedding capacity and generalization for downstream applications such as link predictions over graphs and hierarchy inference. On the other hand, in order to develop **hyperbolic neural networks**, arithmetic such as addition and multiplication in hyperbolic space is required. However, hyperbolic space is not a vector space, so addition and multiplication are not well-defined, making the right methodology unclear. Several different approaches to this problem have been proposed.

Gyrovector space. Existing works including HNN [10], HNN++ [30], HVAE [21], and HGAT [44], adopt the framework of *gyrovector space* as a non-associative algebraic formalism for hyperbolic geometry, by equipping hyperbolic space with non-associative addition and multiplication. This Möbius addition \oplus and Möbius scalar multiplication \otimes , for $\mathbf{x}, \mathbf{y} \in \mathcal{B}^n$ and $r \in \mathbb{R}$ is defined as

$$\mathbf{x} \oplus \mathbf{y} := \frac{(1+2\langle \mathbf{x}, \mathbf{y} \rangle + \|\mathbf{y}\|^2)\mathbf{x} + (1-\|\mathbf{x}\|^2)\mathbf{y}}{1+2\langle \mathbf{x}, \mathbf{y} \rangle + \|\mathbf{x}\|^2\|\mathbf{y}\|^2}, \quad r \otimes \mathbf{x} := \tanh(r \tanh^{-1}(\|\mathbf{x}\|)) \frac{\mathbf{x}}{\|\mathbf{x}\|}.$$

Subsequent operations such as matrix-vector multiplications can be derived analogously to the Euclidean case with these basic operations. However, Möbius addition and scalar multiplication are complicated with a high computation; high level operations such as Möbius matrix-vector multiplication and convolution are even more complicated and numerically unstable due to the use of ill-conditioned functions like \tanh . Also, this approach treats hyperbolic space more as a gyrovector space than as a manifold object, so it can not be generalized to other manifolds that lack this structure.

Push-forward & Pull-backward. Another approach to utilizing the power of hyperbolic geometry is using Push-forward & Pull-backward mappings. Since many commonly used operations are well-defined in Euclidean space but not in hyperbolic space, it is natural to try to map the hyperbolic points to Euclidean space, apply well-defined operations there, then map back to hyperbolic space. Many works, including HATN [12], HGCN [6], HGNN [19], and HGAT [44], propose to

- pull the hyperbolic points to Euclidean space with a “pull-backward” mapping;
- apply operations such as multiplication and convolution in Euclidean space; and then
- push the resulting Euclidean points to hyperbolic space with a “push-forward” mapping.

However, hyperbolic space and Euclidean space are different spaces and as a result, no isomorphic mappings or one-to-one correspondences exist between them. A common choice of the push-forward & pull-backward mapping [6, 19] is the exponential map $\exp_{\mathbf{x}}(\cdot)$ & logarithm map $\log_{\mathbf{x}}(\cdot)$, where \mathbf{x} is usually chosen to be the origin \mathbf{O} . The exponential and logarithm maps are mappings between the hyperbolic space and its tangent space $\mathcal{T}_{\mathbf{x}}\mathbb{H}_n$, which is an Euclidean space that intuitively contains the possible directions in which one can tangentially pass through \mathbf{x} in the hyperbolic space, i.e. where gradients lie. The exponential map maps a vector $\mathbf{v} \in \mathcal{T}_{\mathbf{x}}\mathbb{H}_n$ in the tangent space at \mathbf{x} to another point $\exp_{\mathbf{x}}(\mathbf{v})$ in \mathbb{H}_n (intuitively, $\exp_{\mathbf{x}}(\mathbf{v})$ is the point reached by starting at \mathbf{x} and moving in the direction of \mathbf{v} a distance $\|\mathbf{v}\|$ along the manifold), while the logarithm map inverts this.

This approach is more straightforward and natural in the sense that hyperbolic space is only treated as a manifold object with no more structures added, so it can be generalized to general manifolds. However, even the natural $\exp_{\mathbf{O}}(\cdot)$ and $\log_{\mathbf{O}}(\cdot)$ are still complicated and numerically unstable. Both push-forward and pull-backward mappings are used at every hyperbolic layer, which incurs a high computational complexity in both the model forward and backward loop. As a result, this prevents hyperbolic networks from scaling to large graphs. Moreover, despite its impressive performance on many tasks [6, 19], this approach in some sense is just a Euclidean network with $\exp_{\mathbf{O}}(\cdot)$ and $\log_{\mathbf{O}}(\cdot)$ as two “fancy” nonlinearities, which makes the mechanism behind the model’s success less clear.

Horocycle Features. Perhaps the most similar work to ours is Wang [37], where hyperbolic neuron models are constructed using the *hyperbolic Poisson kernel* $P_n(\mathbf{x}, \boldsymbol{\omega}) = (\frac{1-\|\mathbf{x}\|^2}{\|\mathbf{x}-\boldsymbol{\omega}\|^2})^{n-1}$ for $\mathbf{x} \in \mathcal{B}^n$, $\boldsymbol{\omega} \in \partial\mathcal{B}^n$, which is constant over any horocycle that is tangential to $\partial\mathcal{B}^n$ (i.e., S^{n-1}) at $\boldsymbol{\omega}$. Horocycles are hyperbolic analogs of Euclidean hyperplanes. In the Poincaré disk model \mathcal{B}^n , horocycles are precisely the $(n-1)$ -dimensional spheres that are tangential to $\partial\mathcal{B}^n$ [14]. Wang [37] differs from our simple HyLa approach in that it still uses a push-forward mapping, specifically the exponential map $\exp_{\mathbf{x}}(\cdot)$, in their proposed horocycle multiple linear regression model, together with a more complicated feature function $f_{a,p}^1(\mathbf{x})$ proposed. Another recent related work [33] theoretically proposes a continuous version of shallow fully-connected networks on non-compact symmetric space

(including hyperbolic space) using Helgason-Fourier transform, where the network function shares some similarities to the horocycle features. Specifically, they show that the horocycle features together with a non-Euclidean factor can be a nice “basis” (infinite linear combination) of $L^2(\mathbb{H}_n)$.

3 HyLa: Euclidean Features from Hyperbolic Embeddings

In this section, we describe HyLa, our principled way of using hyperbolic spaces in neural networks, particularly for handling data with graph structure. HyLa uses hyperbolic space once for embedding, then maps immediately to Euclidean features constructed from eigenfunctions of the Laplacian, followed with a modern Euclidean neural network. We start with background on the Laplacian.

Laplace operator (Euclidean). The Laplace operator Δ is defined as the divergence of the gradient of a scalar function f on Euclidean space \mathbb{R}^n , i.e., $\Delta f = \nabla \cdot \nabla f = \sum_{i=1}^n \frac{\partial^2 f}{\partial x_i^2}$. The Laplacian is self-adjoint, and its eigenfunctions are the solutions of the *Helmholtz equation*: $-\Delta f = \lambda f, \lambda \in \mathbb{R}$.

These eigenfunctions are important and useful as they form an *orthonormal basis* for the Hilbert space $L^2(\Omega)$ when $\Omega \in \mathbb{R}^n$ is compact [11]. The eigenspaces of Euclidean Laplacian are spanned by the plane waves $e^{i\langle \omega, x \rangle}$ for $\omega \in \mathbb{R}^n$, where $\langle \cdot, \cdot \rangle$ is the usual inner product.

Theorem 3.1 ([14, 43]). *All smooth eigenfunctions of the Euclidean Laplacian Δ on \mathbb{R}^n are*

$$f(x) = \int_{S^{n-1}} e^{i\lambda \langle \omega, x \rangle} dT(\omega),$$

where $\lambda \in \mathbb{C} - \{0\}$ and T is an analytic functional (or hyperfunction), i.e., an element of the dual space of the space of analytic functions on S^{n-1} .

Therefore, to study the eigenfunctions, it suffices to study the Euclidean plane waves $e^{i\langle \omega, x \rangle}$. The real part of Euclidean plane waves $e^{i\langle \omega, x \rangle}$ are also known in harmonic analysis as Fourier basis functions $x \mapsto \cos(\langle \omega, x \rangle)$, and are used throughout the machine learning literature. For example, these basis functions are used as random Fourier features (RFF) for low-dimensional approximations of kernel functions [24]. The basis function $\cos(\langle \omega, x \rangle)$ can also be adopted as non-linear activation functions in deep neural networks [32, 20, 31].

Laplace-Beltrami operator (Hyperbolic). The Laplace-Beltrami operator \mathcal{L} is the generalization of the Laplace operator to Riemannian manifolds. It is defined as the divergence of the gradient for any twice-differentiable real-valued function f on a Riemannian manifold, i.e., $\mathcal{L}f = \nabla \cdot \nabla f$. We are interested in the Laplace-Beltrami operator in the hyperbolic space [1]. In the n -dimensional Poincaré disk model \mathcal{B}^n , the Laplace-Beltrami operator takes the form

$$\mathcal{L} = \frac{1}{4}(1 - \|x\|^2)^2 \sum_{i=1}^n \frac{\partial^2}{\partial x_i^2} + \frac{n-2}{2}(1 - \|x\|^2) \sum_{i=1}^n x_i \frac{\partial}{\partial x_i}.$$

Motivated by the wide usage and utility of Euclidean Laplacian eigenfunctions, we propose to generalize and derive useful eigenfunctions of the hyperbolic Laplace-Beltrami operator as features, which we call HyLa (for HYperbolic LAPlacian features). This set of real eigenfunctions (HyLa Equation 1) of the Laplace-Beltrami operator will take on the role of the Fourier basis in Euclidean space. In particular, as we will show, any $f \in L^2(\mathbb{H}_n)$ can be expanded as an infinite linear combination (integral form) of these eigenfunctions, letting HyLa express any function.

Hyperbolic Plane Waves and HyLa. There is an entire subspace of infinitely many solutions to the Helmholtz equation and this subspace can be parameterized in many ways. The way we parameterize this subspace matters for learning, as we plan to backpropagate through these eigenfunctions (Section 4). To derive a parameterization, we first consider Euclidean plane waves and assume w is a unit vector ($\|w\| = 1$). Then $e^{i\langle \omega, x \rangle}$ is a plane wave with normal w , i.e., it is constant on each hyperplane perpendicular to w . Here, $\langle \omega, x \rangle$ can be interpreted as the distance of the origin O to the hyperplane $\xi(w, x)$ which passes through x and is perpendicular to w as shown in Figure 1.

Similarly, in hyperbolic space, given a point $z \in \mathcal{B}^n$ in the Poincaré disk model and a unit vector ω , i.e., $\|\omega\| = 1$ and hence $\omega \in \partial \mathcal{B}^n$, the hyperbolic analogue of Euclidean plane wave is $e^{\mu \langle \omega, z \rangle}$, where $\mu \in \mathbb{C}$ and $\langle \omega, z \rangle$ measures the distance of the origin O to some hyperbolic “hyperplane” that

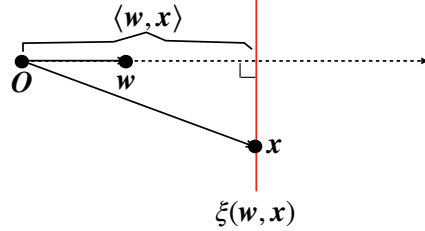


Figure 1: Euclidean hyperplane.

passes through z and is perpendicular to w . The geometric analog of the hyperplane in the Poincaré disk model is the *horocycle*: in Figure 2, the horocycle $\xi(w, z)$ which is perpendicular to w and passes through z , is the Euclidean circle that passes through w, z and is tangential to the boundary $\partial\mathcal{B}^n$ (unit disk) at w . In the Poincaré disk model, the distance from the origin O to the horocycle $\xi(w, z)$ can be computed as $\langle w, z \rangle = \log \frac{1 - \|z\|^2}{\|z - w\|^2} = \log P(z, w)$, where $P(z, w)$ is the Poisson kernel function in two dimensions. If we denote these “hyperbolic plane waves” $e^{\mu\langle w, z \rangle}$ as $e_{\mu, w}(z)$, then it is easy to verify [1] that for $\mu \in \mathbb{C}$, $e_{\mu, w}(z) = e^{\mu\langle w, z \rangle} = P(z, w)^\mu$ and $\mathcal{L}e_{\mu, w} = \mu(\mu - n + 1)e_{\mu, w}$. If we write $\mu = \frac{n-1}{2} + i\lambda$, for $\lambda \in \mathbb{C}$, this yields eigenfunctions $e_{\mu, w}(z) = \exp((\frac{n-1}{2} + i\lambda)\langle w, z \rangle)$ with eigenvalue of $\mu(\mu - n + 1) = -\frac{1}{4}((n-1)^2 + 4\lambda^2)$. Just as the plane waves $e^{i\langle w, x \rangle}$ span the eigenspaces of Euclidean Laplacian, a similar result holds for these “waves” in hyperbolic space.

Theorem 3.2 ([14, 43]). *All smooth eigenfunctions of the Hyperbolic Laplacian \mathcal{L} on \mathcal{B}^n are*

$$f(z) = \int_{\partial\mathcal{B}^n} \exp((i\lambda + \frac{n-1}{2})\langle w, z \rangle) dT(w),$$

where $\lambda \in \mathbb{C}$ and T is an analytic functional (or hyperfunction).

Similar to the Euclidean case, where we are more interested in bounded eigenfunctions of Δ like the Fourier basis functions $x \mapsto \cos(\langle w, x \rangle)$ than we are in eigenfunctions like $x \mapsto \exp(\langle w, x \rangle)$, here we are also interested in eigenfunctions with negative eigenvalues, i.e., $\lambda \in \mathbb{R}$. Unfortunately, the eigenfunctions $e_{\mu, w}(z) = \exp((\frac{n-1}{2} + i\lambda)\langle w, z \rangle)$ are complex when $\lambda \in \mathbb{R}$; we want real eigenfunctions. Fortunately, we can easily get real eigenfunctions from complex ones by observing that the Helmholtz equation for real λ is preserved under complex conjugation, and as a consequence the real part of any of these eigenfunctions $e_{\mu, w}$ (which is just the average of it and its conjugate) will also be an eigenfunction with the same eigenvalue—this will also hold for the real part of $e_{\mu, w}$ scaled by any complex phase $\exp(ib)$. We can write this explicitly for $z \in \mathcal{B}^n$, $w \in \partial\mathcal{B}^n$, $\lambda \in \mathbb{R}$, and $b \in \mathbb{R}$ as

$$\text{HyLa}_{\lambda, b, w}(z) = \text{Re}(\exp(ib) \cdot e_{\mu, w}(z)) = P(z, w)^{\frac{n-1}{2}} \cos(\lambda \log P(z, w) + b). \quad (1)$$

This parameterization, which we call **HyLa** (for **HY**perbolic **L**aplacian features), is the one we will use to produce Euclidean features from hyperbolic embeddings.

HyLa eigenfunctions have the nice property that they are bounded in almost every direction, as $P(z, w)$ approaches 0 as z approaches any point on the boundary of \mathcal{B}^n except w . Another nice property of $e_{\mu, w}$ and HyLa eigenfunctions is that they are invariant to isometries of the space: any isometric transformation of an eigenfunction $e_{\mu, w}$ yields another eigenfunction with the same μ but a transformed w (depending on how the isometry acts on the boundary $\partial\mathcal{B}^n$). Moreover, our derivation of HyLa can be extended naturally to use solutions of the Helmholtz equation on other manifolds (e.g. symmetric spaces) since we only interact with hyperbolic space as a manifold object.

Connection to Euclidean Activation. Here we show a connection between the HyLa eigenfunction and the Euclidean activations used in modern fully connected networks. Given a data point $x \in \mathbb{R}^n$, a weight $w \in \mathbb{R}^n$, a bias $b \in \mathbb{R}$ and nonlinearity σ , the Euclidean activation is $\sigma(\langle w, x \rangle + b) = \sigma(\|w\| \langle \frac{w}{\|w\|}, x \rangle + b)$, where $\langle \frac{w}{\|w\|}, x \rangle$ measures the distance of the origin to the hyperplane $\xi(\frac{w}{\|w\|}, x)$. For $z \in \mathcal{B}^n$, $w \in \partial\mathcal{B}^n$, $\lambda \in \mathbb{R}$, and $b \in \mathbb{R}$, we can reformulate the HyLa eigenfunction as

$$\text{HyLa}_{\lambda, b, w}(z) = \sigma(\lambda \langle w, z \rangle + b) P(z, w)^{\frac{n-1}{2}},$$

where the non-linear function is $\sigma = \cos$ and $\langle w, z \rangle$ measures the distance from the origin O to the horocycle $\xi(w, z)$. From this perspective, HyLa is a straight generalization of Euclidean activations to hyperbolic space, where the extra factor $P(z, w)^{\frac{n-1}{2}}$ arises as a result of curvature of \mathbb{H}_n .

It is natural to ask whether the \cos function can be replaced with general non-linear activation functions such as ReLU. Even though they would not be eigenfunctions anymore, a recent work (Theorem 4.3 in Sonoda et al. [33]) suggests that it is possible and reasonable to use some other non-linear activations including ReLU in HyLa, particularly due to the result that any $f \in L^2(\mathbb{H}_n)$ can be expanded as an infinite linear combination (integral form) of HyLa (Equation 1) modified to have σ be any a tempered distribution on \mathbb{R} , i.e., the topological dual of the Schwartz test functions, including ReLU and \cos . For simplicity, here we use \cos in HyLa functions unless specified otherwise.

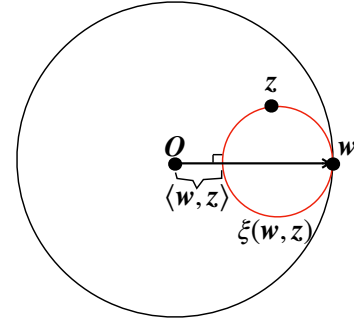


Figure 2: Hyperbolic horocycle.

4 HyLa for Graph Learning

Background on Graph Learning. A graph is defined formally as $\mathcal{G} = (\mathcal{V}, \mathbf{A})$, where \mathcal{V} represents the vertex set consisting of n nodes and $\mathbf{A} \in \mathbb{R}^{n \times n}$ represents the symmetric adjacency matrix. Besides the graph structure, in graph learning each node in the graph has a corresponding d -dimensional feature vector: we let $\mathbf{X} \in \mathbb{R}^{n \times d}$ denote the entire feature matrix for all nodes. A fraction of nodes are associated with a label indicating one (or multiple) categories it belongs to. The *node classification* task is to predict the labels of nodes without labels or even of nodes newly added to the graph.

A GCN [18, 9] layer takes \mathbf{A} and \mathbf{X} as inputs, and outputs $f(\mathbf{A}, \mathbf{X})$ as new node representations to the next layer. f consists of three stages: feature propagation, linear transformation, and a nonlinear activation. In the feature propagation stage, the features of each node are averaged with the features of connected nodes. We can formalize this process using the “normalized” adjacency matrix \mathbf{S} with added self-loops: $\mathbf{S} = \tilde{\mathbf{D}}^{-1/2} \tilde{\mathbf{A}} \tilde{\mathbf{D}}^{-1/2}$, where $\tilde{\mathbf{A}} = \mathbf{A} + \mathbf{I}$ and $\tilde{\mathbf{D}}$ is the corresponding degree matrix. The feature propagation for all nodes can then be described as $\mathbf{S}\mathbf{X}$, which encourages nodes in the same category to have similar features by propagating through connected edges. In the following stages, a GCN layer acts as a standard linear layer \mathbf{W} with a non-linear activation function such as ReLU. Hence, we can write $f(\mathbf{A}, \mathbf{X}) = \text{ReLU}(\mathbf{S}\mathbf{X}\mathbf{W})$. A deep GCN consists of a stack of multiple GCN layers. For classification tasks, the last layer of GCN outputs the probabilities of nodes belonging to a category with a softmax classifier.

An interesting work to understand GCN is *simplifying GCN* (SGC) [38], where the authors remove the non-linearities in GCN and derive a simple version as: $f(\mathbf{A}, \mathbf{X}) = \text{softmax}(\mathbf{S}^K \mathbf{X}\mathbf{W})$. This is essentially a multi-class logistic regression on the pre-processed features $\mathbf{S}^K \mathbf{X}$. Note that these features can be computed before training. Surprisingly, this simplification does not seem to hurt the performance of GCN, and it enables large graph learning and greatly saves memory and computation cost. Empirical results of SGC match and rival the performance of a GCN model in node classification and a series of downstream tasks.

End-to-End Learning with HyLa. We now give a full recipe for using HyLa for graph learning. In a graph learning task, we assume the adjacent matrix $\mathbf{A} \in \mathbb{R}^{n \times n}$ is given, sometimes together with a node representation feature matrix $\mathbf{X} \in \mathbb{R}^{n \times d}$. The high-level idea of using HyLa is simple. We initialize an embedding in hyperbolic space for each object (e.g. nodes in the graph), from which we derive Euclidean features using HyLa functions, which is then used with any graph neural networks $f(\mathbf{A}, \mathbf{X})$. Both the graph neural network parameters and the embedding points are allowed to be learned. HyLa can be used at both node level and feature level as detailed below.

Node level. When used at node level, we initialize a low dimensional hyperbolic embedding $\mathbf{z} \in \mathcal{B}^{d_0}$ for each node to derive hyperbolic embeddings $\mathbf{Z} \in \mathbb{R}^{n \times d_0}$ for all nodes in the graph, from which we derive Euclidean features $\mathbf{H} \in \mathbb{R}^{n \times d_1}$ using HyLa functions. We replace (or concatenate) the original node feature matrix \mathbf{X} with \mathbf{H} as the new node feature matrix $\bar{\mathbf{X}}$. Using HyLa at node level is better-suited for tasks where no feature matrix is available or meaningful features are hard to derive. However, the size of \mathbf{Z} will be proportional to the size of the graph, hence it cannot scale to very large graphs due to memory and computation constraints. Further more, this method can only be used in a transductive setting, where nodes in the test set are seen during training.

Feature level. When used at feature level, we initialize a low dimensional hyperbolic embedding $\mathbf{z} \in \mathcal{B}^{d_0}$ for each dimension of feature to derive hyperbolic embeddings $\mathbf{Z} \in \mathbb{R}^{d \times d_0}$ for all features, from which we derive Euclidean features $\mathbf{H} \in \mathbb{R}^{d \times d_1}$ using HyLa functions. We then adopt $\bar{\mathbf{X}} = \mathbf{X}\mathbf{H}$ as the new node feature matrix since HyLa features are built for each dimension of feature. The dimension d of the original feature matrix is usually fixed and much lower than the number of nodes n in a graph, so HyLa at feature level can be used even for large graphs. Since the hyperbolic embeddings are built for each feature dimension, it can be used in both transductive and inductive settings, as long as the test data shares the same set of features as the training data. One limitation of this method is that its performance depends on the existence of a feature matrix \mathbf{X} that contains sufficient information for learning.

End-to-end learning. In either the node-level or feature-level case, an end-to-end model can be formalized as $f(\mathbf{A}, \bar{\mathbf{X}})$, where $\bar{\mathbf{X}}$ is derived from hyperbolic embeddings \mathbf{Z} using HyLa function. In our experiment, we use HyLa together with the linear graph network SGC, which takes the form $f(\mathbf{A}, \bar{\mathbf{X}}) = \text{softmax}(\mathbf{A}^K \bar{\mathbf{X}}\mathbf{W})$ with a trainable weight matrix \mathbf{W} . Note that just as the vanilla SGC

Table 1: Node classification Dataset statistics.

Setting	Dataset	# Nodes	# Edges	Classes	Features
Trans- ductive	Cora	2,708	5,429	7	1,433
	Citeseer	3,327	4,732	6	3,703
	Pubmed	19,717	44,338	3	500
	Disease	1,044	1,043	2	1,000
	Airport	3,188	18,631	4	4
Inductive	Reddit	233K	11.6M	41	602

Table 2: Text classification Dataset statistics.

Dataset	# Docs	# Words	Average Length	Classes
R8	7,674	7688	65.72	8
R52	9,100	8892	69.82	52
Ohsumed	7400	14157	135.82	23
MR	10662	18764	20.39	2

case, \mathbf{A}^K or $\mathbf{A}^K \mathbf{X}$ can be pre-computed in the same way before training and inference. We provide Algorithm 1 as a way to deploying HyLa to an end-to-end graph learning system. More training details can be found in Appendix.

5 Experiments

5.1 Node Classification

Task and Datasets. In the semi-supervised node classification task, the goal is to classify each node into a correct category. We use both transductive and inductive datasets detailed in Table 1. Cora, Citeseer and Pubmed [29] are standard **citation networks** benchmarks, where nodes represent papers, connected to each other via citations. We follow the standard splits adopted in [18, 38]. **Disease propagation tree** [6] is tree networks simulating the SIR disease spreading model [2], where the label is whether a node was infected or not and the node features indicate the susceptibility to the disease. **Airport** dataset [6] is a transductive dataset where nodes represent airports and edges represent the airline routes as from OpenFlights. Nodes’ labels are chosen to be the population of the country where the airport belongs to. We supplement our experiment by predicting community structure on an inductive dataset Reddit following [38], which consists of a much larger graph. More details of datasets (split) are provided in Appendix.

Experiment Setup. All our datasets have node features, so we use HyLa at feature level most of the time, since it applies to both small & large graphs and transductive & inductive tasks. The only exception is the Airport dataset, which only contains 4 dimensional features, hence we use HyLa at node level for Airport to produce better HyLa features. We initialize a hyperbolic embedding $\mathbf{Z} \in \mathbb{R}^{n \times d_0}$ for each feature dimension. We randomly sample d_1 boundary points over the boundary (i.e. $\partial \mathcal{B}^n$) and follow HyLa Algorithm 1 to get the resulting new node features $\bar{\mathbf{X}}$. We use SGC model with HyLa as $\text{softmax}(\mathbf{A}^K \bar{\mathbf{X}} \mathbf{W})$, where both \mathbf{W} and \mathbf{Z} are learned. Further training details are provided in Appendix, our code is available at github¹

Baselines. On Disease, Airport, Pubmed, Citeseer and Cora dataset, we compare our HyLa-SGC model against GCN [18], SGC [38], GAT [35], HGCN [6] and HNN [10] using the publicly released version in Table 8. We tune the hidden dimension by hand. For Reddit dataset, we compare to the reported performance of GaAN, supervised and unsupervised variants of GraphSAGE [13], SGC [38] and FastGCN [7] in Table 8. Note that GCN and HGCN can not be trained on the Reddit dataset because the whole adjacency matrix is too large to fill into memory. Worthy to mention, the HyLa-SGC model can also be designed to train in a batch by batch way for datasets that are even larger than Reddit in case of OOM.

¹<https://github.com/ydydr/HyLa.git>

Table 3: Test accuracy/Micro F1 Score (%) averaged over 10 runs on node classification task. Performance of some baselines are taken from their original papers. **OOM**: Out of memory.

Dataset	Disease	Airport	Pubmed	Citeseer	Cora	Model	Test F1
Hyperbolicity δ	0	1.0	3.5	5.0	11		
GCN	69.7 \pm 0.4	81.4 \pm 0.6	78.1 \pm 0.2	70.5 \pm 0.8	81.3 \pm 0.3	GaAN	96.4
SGC	69.5 \pm 0.2	80.6 \pm 0.1	78.9 \pm 0.0	71.9 \pm 0.1	81.0 \pm 0.0	SAGE-mean	95.0
HGCN	74.5 \pm 0.9	90.6 \pm 0.2	80.3 \pm 0.3	64.0 \pm 0.6	79.9 \pm 0.2	SAGE-GCN	93.0
GAT	70.4 \pm 0.4	81.5 \pm 0.3	79.0 \pm 0.3	72.5 \pm 0.7	83.0 \pm 0.7	FastGCN	93.7
HNN	41.0 \pm 1.8	80.5 \pm 0.5	69.8 \pm 0.4	52.0 \pm 1.0	54.6 \pm 0.4	GCN	OOM
HyLa-SGC	87.0 \pm 1.8	95.0 \pm 0.7	81.0 \pm 0.4	72.6 \pm 0.7	83.0 \pm 0.3	HGCN	OOM
						SGC	94.9
						HyLa-SGC	94.5

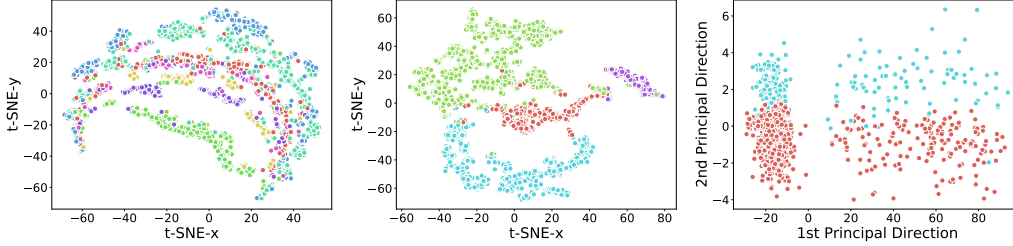


Figure 3: Visualization of node HyLa features on Cora, Airport and Disease datasets, where nodes of different classes are indicated by different colors. (left) t-SNE on Cora; (middle) t-SNE on Airport; (right) PCA on Disease.

Results. From our results in Table 8, we conclude that HyLa is particularly strong and expressive for graph learning. Together with the linear SGC, HyLa-SGC outperforms state-of-the-art GCN models on most datasets. On the Cora dataset, HyLa-SGC beats vanilla SGC and GCN/HGCN and can match the performance of GAT. Particularly for the tree network disease with lowest hyperbolicity (more hyperbolic), the improvements of HyLa-SGC over the SOTA HGCN is about 12.5%! The results suggest that the more hyperbolic the graph is, the more improvements will be gained with HyLa. On Reddit dataset, Table 8 shows that HyLa-SGC outperforms the sampling-based GCN variants, SAGE-GCN and FastGCN by more than 1%. However, the performance is close to SGC, which may indicate that the extra weights and nonlinearities are unnecessary for this particular dataset.

Visualization. In Figure 3, we visualize the learned node HyLa features on Cora, Airport and Disease datasets with t-SNE [34] and PCA projection. This shows that HyLa achieves great label class separation (indicated by different colors) for visualization.

5.2 Text Classification

Task and Datasets. We further evaluate HyLa on **transductive** and **inductive** text classification task to assign labels to documents. We conducted experiments on 4 standard benchmarks including R52 and R8 of Reuters 21578 dataset, Ohsumed and Movie Review (MR) follows the same data split as [40, 38]. Detailed dataset statistics are provided in Table 2.

Experiment Setup. In the transductive case, previous work [40] and Wu et al. [38] apply GCN and SGC by creating a corpus-level graph where both documents and words are treated as nodes at the same level in the graph. For the weights and connections in the graph, word-word edge weights are calculated as pointwise mutual information (PMI) and word-document edge weights as normalized TF-IDF scores. The weights of document-document edges are unknown and left as 0. We follows the same data processing setup for the transductive setting, and adopt HyLa at node level since only adjacent matrix is available.

In the inductive setting, we take the sub-matrix of the large matrix in the transductive setting, including only the document-word edges as the node representation feature matrix \mathbf{X} , then follow the procedure in Section 4 to adopt HyLa at the feature level to get $\bar{\mathbf{X}}$. Particularly in the inductive setting, the adjacency matrix of documents is unknown, we replace SGC with a logistic regression layer (LR) follows HyLa directly as $\mathbf{Y} = \text{softmax}(\bar{\mathbf{X}}\mathbf{W})$. We train the HyLa-SGC & HyLa-LR model for a maximum of 200 epochs and compare it against TextSGC and TextGCN in Table 4.

Table 4: Test accuracy (%) averaged over 10 runs on transductive and inductive text classification task except from the LR mode. **Bold** numbers: best in both transductive and inductive setting; Underlined numbers: best in inductive setting.

Setting	Methods	R8	R52	Ohsumed	MR
Trans- ductive	TextGCN	97.1 \pm 0.1	93.5 \pm 0.2	68.4 \pm 0.6	76.7 \pm 0.2
	TextSGC	97.2 \pm 0.1	94.0 \pm 0.2	68.5 \pm 0.3	75.9 \pm 0.3
	HyLa-SGC	96.9 \pm 0.4	94.1 \pm 0.3	67.3 \pm 0.5	76.2 \pm 0.3
Inductive	TextGCN	95.8 \pm 0.3	88.2 \pm 0.7	57.7 \pm 0.4	74.8 \pm 0.3
	LR	93.3	85.6	56.6	73.0
	HyLa-LR	97.4 \pm 0.2	<u>93.5 \pm 0.2</u>	<u>64.9 \pm 0.3</u>	<u>75.5 \pm 0.3</u>

Performance Analysis. In the transductive setting when HyLa is adopted at node level, it can match the performance of TextGCN and TextSGC. The corpus-level graph may contain sufficient information to learn the task, and hence HyLa-SGC does not seem to outperform them, but still has a comparable performance. HyLa shows extraordinary performance in the inductive setting when used at feature level, together with a linear regression model it can already outperform inductive TextGCN, sometimes even better than the performance of a transductive TextGCN model, which indicates that there is redundant information in the corpus-level graph.

From the results on the inductive text classification task, we argue that HyLa (at feature level) is particularly useful in the following three ways. First, it can solve the OOM problem of classic GCN model in large graphs, and requires less memory during training, since there are limited number of lower level features (also \mathbf{X} is usually sparse), and there is no need to build a corpus-level graph anymore. Second, it is naturally inductive as HyLa is built at feature level (for each word in this task), it generalizes to any unseen new nodes (documents) that uses the same set of features (words). Third, the model is simple: HyLa follows by a linear regression model, which computes faster and easier than classical GCN models.

Efficiency. Following Wu et al. [38], we measure the training time of HyLa-based models on the Pubmed dataset, and we compare against state-of-the-arts graph networks including SGC, GCN, GAT, HGCN and HNN. In Figure 4, we plot the timing performance of various models. In particular, we take into account the pre-computation time of some models into training time. We measure the training time on a NVIDIA GeForce RTX 2080 Ti GPU and show the specific timing statistics in Appendix.

Particularly for HGCN model, in order to achieve the report performances, we follow the same training procedure using public code, which is divided into two stages: (1) a link prediction task on the dataset to learn hyperbolic embeddings, and (2) use the pretrained embeddings to train a MLP classifier. Hence, we add the timing of both stages as the timing for HGCN. Figure 3 shows that HyLa-based models achieves the best performance while incurring a minor computational slowdown, which is $4.4\times$ faster than HGCN.

We also performed an ablation study comparing HyLa with ReLU and cos activations and comparing HyLa with Euclidean RFF. For want of space, we defer this to the Appendix.

6 Conclusion

We propose a simple and efficient approach to using hyperbolic space in neural networks, by theoretically deriving HyLa as an expressive feature using the eigenfunctions of Laplacian in the hyperbolic space. Empirical results from adopting HyLa on graph learning tasks show that HyLa can outperform SOTA hyperbolic networks. HyLa sheds light as a principled approach to utilizing hyperbolic geometry in neural networks in an entirely different way to previous work. Possible future directions include (1) using HyLa with non-linear graph networks such as GCN to derive even

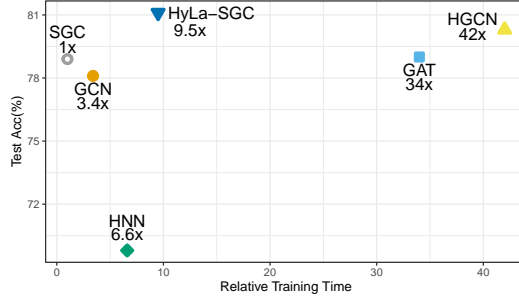


Figure 4: Performance over training time on Pubmed. HyLa-SGC achieves best performance with minor computation slowdown.

more expressive models; and (2) adopting more numerically stable representations of the hyperbolic embeddings to avoid potential “NaN problems” when running HyLa-based models.

References

- [1] Shmuel Agmon. On the spectral theory of the laplacian on noncompact hyperbolic manifolds. *Journées Équations aux dérivées partielles*, pages 1–16, 1987.
- [2] Roy M Anderson and Robert M May. *Infectious diseases of humans: dynamics and control*. Oxford university press, 1992.
- [3] Silvere Bonnabel. Stochastic gradient descent on riemannian manifolds. *IEEE Transactions on Automatic Control*, 58(9):2217–2229, 2013.
- [4] Brian H Bowditch. A course on geometric group theory. 2006.
- [5] James W Cannon, William J Floyd, Richard Kenyon, Walter R Parry, et al. Hyperbolic geometry. *Flavors of geometry*, 31(59-115):2, 1997.
- [6] Ines Chami, Zhitao Ying, Christopher Ré, and Jure Leskovec. Hyperbolic graph convolutional neural networks. *Advances in neural information processing systems*, 32:4868–4879, 2019.
- [7] Jie Chen, Tengfei Ma, and Cao Xiao. Fastgcn: fast learning with graph convolutional networks via importance sampling. *arXiv preprint arXiv:1801.10247*, 2018.
- [8] Wei Chen, Wenjie Fang, Guangda Hu, and Michael W Mahoney. On the hyperbolicity of small-world and treelike random graphs. *Internet Mathematics*, 9(4):434–491, 2013.
- [9] Michaël Defferrard, Xavier Bresson, and Pierre Vandergheynst. Convolutional neural networks on graphs with fast localized spectral filtering. *Advances in neural information processing systems*, 29:3844–3852, 2016.
- [10] Octavian-Eugen Ganea, Gary Bécigneul, and Thomas Hofmann. Hyperbolic neural networks. *arXiv preprint arXiv:1805.09112*, 2018.
- [11] David Gilbarg and Neil S Trudinger. *Elliptic partial differential equations of second order*, volume 224. springer, 2015.
- [12] Caglar Gulcehre, Misha Denil, Mateusz Malinowski, Ali Razavi, Razvan Pascanu, Karl Moritz Hermann, Peter Battaglia, Victor Bapst, David Raposo, Adam Santoro, et al. Hyperbolic attention networks. *arXiv preprint arXiv:1805.09786*, 2018.
- [13] William L Hamilton, Rex Ying, and Jure Leskovec. Inductive representation learning on large graphs. In *Proceedings of the 31st International Conference on Neural Information Processing Systems*, pages 1025–1035, 2017.
- [14] Sigurdur Helgason. *Groups and geometric analysis: integral geometry, invariant differential operators, and spherical functions*, volume 83. American Mathematical Society, 2022.
- [15] Peter D Hoff, Adrian E Raftery, and Mark S Handcock. Latent space approaches to social network analysis. *Journal of the american Statistical association*, 97(460):1090–1098, 2002.
- [16] Dhiraj Kalamkar, Dheevatsa Mudigere, Naveen Mellempudi, Dipankar Das, Kunal Banerjee, Sasikanth Avancha, Dharma Teja Vooturi, Nataraj Jammalamadaka, Jianyu Huang, Hector Yuen, et al. A study of bfloat16 for deep learning training. *arXiv preprint arXiv:1905.12322*, 2019.
- [17] Diederik P Kingma and Jimmy Ba. Adam: A method for stochastic optimization. *arXiv preprint arXiv:1412.6980*, 2014.
- [18] Thomas N Kipf and Max Welling. Semi-supervised classification with graph convolutional networks. *arXiv preprint arXiv:1609.02907*, 2016.
- [19] Qi Liu, Maximilian Nickel, and Douwe Kiela. Hyperbolic graph neural networks. *arXiv preprint arXiv:1910.12892*, 2019.

- [20] Chunjie Luo, Jianfeng Zhan, Xiaohe Xue, Lei Wang, Rui Ren, and Qiang Yang. Cosine normalization: Using cosine similarity instead of dot product in neural networks. In *International Conference on Artificial Neural Networks*, pages 382–391. Springer, 2018.
- [21] Emile Mathieu, Charline Le Lan, Chris J Maddison, Ryota Tomioka, and Yee Whye Teh. Continuous hierarchical representations with poincaré variational auto-encoders. *Advances in neural information processing systems*, 32, 2019.
- [22] Maximillian Nickel and Douwe Kiela. Poincaré embeddings for learning hierarchical representations. *Advances in neural information processing systems*, 30:6338–6347, 2017.
- [23] Maximillian Nickel and Douwe Kiela. Learning continuous hierarchies in the lorentz model of hyperbolic geometry. In *International Conference on Machine Learning*, pages 3779–3788. PMLR, 2018.
- [24] Ali Rahimi, Benjamin Recht, et al. Random features for large-scale kernel machines. In *NIPS*, volume 3, page 5. Citeseer, 2007.
- [25] Erzsébet Ravasz and Albert-László Barabási. Hierarchical organization in complex networks. *Physical review E*, 67(2):026112, 2003.
- [26] Ryan Rossi and Nesreen Ahmed. The network data repository with interactive graph analytics and visualization. In *Twenty-Ninth AAAI Conference on Artificial Intelligence*, 2015.
- [27] Frederic Sala, Chris De Sa, Albert Gu, and Christopher Ré. Representation tradeoffs for hyperbolic embeddings. In *International conference on machine learning*, pages 4460–4469. PMLR, 2018.
- [28] Rik Sarkar. Low distortion delaunay embedding of trees in hyperbolic plane. In *International Symposium on Graph Drawing*, pages 355–366. Springer, 2011.
- [29] Prithviraj Sen, Galileo Mark Namata, Mustafa Bilgic, Lise Getoor, Brian Gallagher, and Tina Eliassi-Rad. Collective classification in network data. *AI Magazine*, 29(3):93–106, 2008.
- [30] Ryohei Shimizu, Yusuke Mukuta, and Tatsuya Harada. Hyperbolic neural networks++. *arXiv preprint arXiv:2006.08210*, 2020.
- [31] P Sibi, S Allwyn Jones, and P Siddarth. Analysis of different activation functions using back propagation neural networks. *Journal of theoretical and applied information technology*, 47(3): 1264–1268, 2013.
- [32] Vincent Sitzmann, Julien Martel, Alexander Bergman, David Lindell, and Gordon Wetzstein. Implicit neural representations with periodic activation functions. In H. Larochelle, M. Ranzato, R. Hadsell, M. F. Balcan, and H. Lin, editors, *Advances in Neural Information Processing Systems*, volume 33, pages 7462–7473. Curran Associates, Inc., 2020. URL <https://proceedings.neurips.cc/paper/2020/file/53c04118df112c13a8c34b38343b9c10-Paper.pdf>.
- [33] Sho Sonoda, Isao Ishikawa, and Masahiro Ikeda. Fully-connected network on noncompact symmetric space and ridgelet transform based on helgason-fourier analysis. *arXiv preprint arXiv:2203.01631*, 2022.
- [34] Laurens Van der Maaten and Geoffrey Hinton. Visualizing data using t-sne. *Journal of machine learning research*, 9(11), 2008.
- [35] Petar Veličković, Guillem Cucurull, Arantxa Casanova, Adriana Romero, Pietro Lio, and Yoshua Bengio. Graph attention networks. *arXiv preprint arXiv:1710.10903*, 2017.
- [36] Petar Velickovic, William Fedus, William L Hamilton, Pietro Liò, Yoshua Bengio, and R Devon Hjelm. Deep graph infomax. *ICLR (Poster)*, 2(3):4, 2019.
- [37] Ming-Xi Wang. Laplacian eigenspaces, horocycles and neuron models on hyperbolic spaces. 2020.

- [38] Felix Wu, Amauri Souza, Tianyi Zhang, Christopher Fifty, Tao Yu, and Kilian Weinberger. Simplifying graph convolutional networks. In *International conference on machine learning*, pages 6861–6871. PMLR, 2019.
- [39] Keyulu Xu, Weihua Hu, Jure Leskovec, and Stefanie Jegelka. How powerful are graph neural networks? *arXiv preprint arXiv:1810.00826*, 2018.
- [40] Liang Yao, Chengsheng Mao, and Yuan Luo. Graph convolutional networks for text classification. In *Proceedings of the AAAI conference on artificial intelligence*, volume 33, pages 7370–7377, 2019.
- [41] Tao Yu and Chris De Sa. Numerically accurate hyperbolic embeddings using tiling-based models. *Advances in neural information processing systems*, 2019.
- [42] Tao Yu and Christopher M De Sa. Representing hyperbolic space accurately using multi-component floats. *Advances in Neural Information Processing Systems*, 34, 2021.
- [43] Steve Zelditch. *Eigenfunctions of the Laplacian on a Riemannian manifold*, volume 125. American Mathematical Soc., 2017.
- [44] Yiding Zhang, Xiao Wang, Chuan Shi, Xunqiang Jiang, and Yanfang Fanny Ye. Hyperbolic graph attention network. *IEEE Transactions on Big Data*, 2021.

Table 5: Hyper-parameters for node classification.

Dataset	d_0	d_1	K	s	lr_1	lr_2	# Epochs	Early Stopping
Disease	25	500	2	0.1	0.05	0.0001	100	<i>No</i>
Airport	50	1000	2	0.01	0.1	0.1	100	<i>No</i>
Pubmed	50	1000	10	0.01	0.1	0.01	200	<i>Yes</i>
Citeseer	50	1000	5	0.1	0.001	0.0001	100	<i>Yes</i>
Cora	50	250	2	0.5	0.01	0.01	100	<i>No</i>
Reddit	50	1000	2	0.5	0.1	0.001	100	<i>No</i>

A Experiment Details

A.1 Task and Dataset

We provide below a detailed description of datasets used in the text classification task.

1. **Citation Networks.** Cora, Citeseer and Pubmed [29] are standard citation network benchmarks, where nodes represent papers, connected to each other via citations. We follow the standard splits [18] with 20 nodes per class for training, 500 nodes for validation and 1000 nodes for test.
2. **Disease propagation tree** [6]. This is tree networks simulating the SIR disease spreading model [2], where the label is whether a node was infected or not and the node features indicate the susceptibility to the disease. We use dataset splits of 30/10/60% for train/val/test set.
3. **Airport.** We take this dataset from [6]. This is a transductive dataset where nodes represent airports and edges represent the airline routes as from OpenFlights. Airport contains 3,188 nodes, each node has a 4 dimensional feature representing geographic information (longitude, latitude and altitude), and GDP of the country where the airport belongs to. For node classification, labels are chosen to be the population of the country where the airport belongs to. We use dataset splits of 524/524 nodes for val/test set.
4. **Reddit.** This is a much larger graph dataset built from Reddit posts, where the label is the community, or “subreddit”, that a post belongs to. Two nodes are connected if the same user comments on both. We use a dataset split of 152K/24K/55K follows [13, 7], similarly, we evaluate HyLa inductively by following [38]: we train on a subgraph comprising only training nodes and test with the original graph.

A.2 Training details.

We use HyLa together with SGC model as $\text{softmax}(\mathbf{A}^K \bar{\mathbf{X}} \mathbf{W})$, where the HyLa feature matrix $\bar{\mathbf{X}} \in \mathbb{R}^{n \times d_1}$ is derived from the hyperbolic embedding $\mathbf{Z} \in \mathbb{R}^{n \times d_0}$ using Algorithm 1. Specifically, we randomly sample constants of HyLa features $\bar{\mathbf{X}}$ by sampling the boundary points ω uniformly from the boundary $\partial \mathcal{B}^n$, eigenvalue constants λ from a zero-mean s -standard-deviation Gaussian and biases b uniformly from $[0, 2\pi]$. These constants remain fixed throughout training.

We use cross-entropy as the loss function and jointly optimize the low dimensional hyperbolic embedding \mathbf{Z} and linear weight \mathbf{W} simultaneously during training. Specifically, Riemannian SGD optimizer [3] (of learning rate lr_1) for \mathbf{Z} and Adam [17] optimizer (of learning rate lr_2) for \mathbf{W} . RSGD naturally scales to very large graph because the graph connectivity pattern is sufficiently sparse. We adopt early-stopping for Adam optimizer as regularization. We tune the hyper-parameter via grid search over the parameter space. Each hyperbolic embedding is initialized around the origin, by sampling each coordinate at random from $[-10^{-5}, 10^{-5}]$.

A.3 Hyper-parameters

We provide the detailed values of hyper-parameters for **node classification** and **text classification** in Table 5 and Table 6 respectively. Particularly, we fix $K = 2$ for the text classification task and train the model for a maximum of 200 epochs without using any regularization (e.g. early stopping). Also note that in the transductive text classification setting, HyLa is used at node level, hence the

Table 6: Hyper-parameters for text classification.

Dataset	Transductive Setting					Inductive Setting				
	d_0	d_1	s	lr_1	lr_2	d_0	d_1	s	lr_1	lr_2
R8	50	500	0.5	0.01	0.0001	50	500	0.5	0.001	0.0001
R52	50	500	0.5	0.1	0.0001	50	1000	0.5	0.008	0.0001
Ohsumed	50	500	0.5	0.01	0.0001	50	1000	0.1	0.001	0.0001
MR	30	500	0.5	0.1	0.0001	50	500	0.5	0.01	0.0001

size of parameters will be proportional to the size of graph, in which case, d_0 and d_1 can not be too large so as to avoid OOM. In the inductive text classification setting, there is no such constraint as the dimension of lower level features is not very large itself. Please check the code for more details.

B Timing

We show the specific training timing statistics of different models on Pubmed dataset in Table 7.

Table 7: Training time on Pubmed.

Model	Timing (seconds)
SGC	0.3685
GCN	1.2468
GAT	12.5179
HNN	2.4146
HGCN	OOM
HyLa-SGC	3.5102

C Ablation Study

Comparison to Euclidean space. As HyLa uses the eigenfunctions of the Laplace-Beltrami operator, a natural comparison is to the eigenfunctions of the Laplacian in the Euclidean space, i.e. random Fourier features (RFF) for some Euclidean embeddings. Hence, we also implement the RFF-based models, i.e. RFF-SGC model ($\mathbf{A}^K \mathbf{R} \mathbf{W}$) and RFF-LR model ($\mathbf{X} \mathbf{R} \mathbf{W}$) as an ablation study, where \mathbf{R} is the random Fourier feature matrix of Euclidean embeddings. This approach is essentially identical to HyLa, with the hyperbolic space swapped out for Euclidean space. We conduct experiments on the node classification task, where HyLa consistently outperforms RFF, significantly on more hyperbolic datasets (Disease with 3.9%) and mildly on less hyperbolic datasets (Cora with 0.8%). RFF only slightly outperforms HyLa with 0.5% on the MR dataset. This shows the utility of embedding in hyperbolic space. It is worth mentioning that although HyLa consistently outperforms the RFF approach, in some tasks (such as disease), RFF is already enough to outperform some of the previous work.

Table 8: Test accuracy/Micro F1 Score (%) averaged over 10 runs on node classification task. Performance of some baselines are taken from their original papers. **OOM**: Out of memory.

Dataset	Disease	Airport	Pubmed	Citeseer	Cora
Hyperbolicity δ	0	1.0	3.5	5.0	11
RFF-SGC	83.1 \pm 0.7	94.8 \pm 0.8	78.1 \pm 0.4	66.6 \pm 0.4	82.2 \pm 0.5
HyLa(cos)-SGC	87.0 \pm 1.8	95.0 \pm 0.7	81.0 \pm 0.4	72.6 \pm 0.7	83.0 \pm 0.3